ENERGY CONSERVATION

ORNL/CON-318

EVALUATION OF POTENTIAL PERFORMANCE ADDITIVES FOR THE ADVANCED LITHIUM BROMIDE CHILLER

R. H. Reiner
W. Del Cul
H. Perez-Blanco
M. R. Ally
A. Zaltash

April 1991

Thermally Activated Heat Pump Research
DOE/ORNL Building Equipment Research Program
Oak Ridge National Laboratory

Prepared by the
OAK RIDGE NATIONAL LABORATORY
managed by
MARTIN MARIETTA ENERGY SYSTEMS, INC.
Oak Ridge, Tennessee 37831-6285
for the
U. S. DEPARTMENT OF ENERGY
under Contract No. DE-AC05-84OR21400

ORNL/CON-318

EVALUATION OF POTENTIAL PERFORMANCE ADDITIVES FOR THE ADVANCED LITHIUM BROMIDE CHILLER

R. H. Reiner
W. Del Cul
H. Perez-Blanco
M. R. Ally
A. Zaltash

April 1991

Thermally Activated Heat Pump Research
DOE/ORNL Building Equipment Research Program
Oak Ridge National Laboratory

Prepared by the
OAK RIDGE NATIONAL LABORATORY
managed by
MARTIN MARIETTA ENERGY SYSTEMS, INC.
Oak Ridge, Tennessee 37831-6285
for the
U. S. DEPARTMENT OF ENERGY
under Contract No. DE-AC05-84OR21400

TABLE OF CONTENTS

LIST OF FIGURES v

LIST OF TABLES vii

ACKNOWLEDGMENTS ix

ABSTRACT xi

NOMENCLATURE xiii

1. INTRODUCTION 1

2. EXPERIMENTAL PROCEDURE AND DESCRIPTION 3
- 2.1 Static Performance Screening 3
- 2.2 Dynamic Performance Testing 3
- 2.3 Stability Measurements 5

3. RESULTS 7
- 3.1 Static Performance Enhancement Results 7
- 3.2 Dynamic Performance Enhancement Results 12
- 3.3 Thermal and Chemical Stability Results 14

4. DISCUSSION 19
- 4.1 Static Performance Enhancement 19
- 4.2 Dynamic Performance Enhancement 19
- 4.3 Thermal and Chemical Stability 20
- 4.4 Implications for Advanced Chiller Development 21

5. CONCLUSIONS 23

REFERENCES 25

LIST OF FIGURES

Fig. 1. Schematic of minisorber apparatus used to evaluate performance additive effectiveness. 4
Fig. 2. Performance (mass transfer) enhancement, E, as a function of 2-ethyl-1-hexanol concentration, [2EH], in a static pool of aqueous LiBr. 8
Fig. 3. Performance (heat transfer) enhancement, E_H, as a function of 2-ethyl-1-hexanol concentration, [2EH], in a falling film absorber. 13
Fig. 4. Thermal stability of 2EH (2-ethyl-1-hexanol) obtained by DSC (differential scanning calorimetry). 15
Fig. 5. Chemical stability of 1-heptanol(HEP)-chromate mixture obtained by DSC (differential scanning calorimetry). 16

LIST OF TABLES

Table 1. Performance (mass transfer) enhancement, E, as a function of 2-ethyl-1-hexanol concentration, [2EH] 7
Table 2. Static performance enhancement, E, as a function of 1-heptanol concentration, [HEP] 9
Table 3. Static performance enhancement, E, as a function of 1H,1H,7H-dodecafluoro-1-heptanol concentration, [DFH] 9
Table 4. Static performance enhancement, E, as a function of 1,1,1-trifluoro-2-octanol concentration, [TFO] 10
Table 5. Maximum static enhancement, $E_{M,}$ of various additives 11
Table 6. Comparison of performance enhancement, $E_{M,}$ with mechanical stirring and performance additives 11
Table 7. Effect of additive combination on performance enhancement 12
Table 8. Minisorber performance enhancement of various additives 14
Table 9. Stability of performance additives in various environments 16

ACKNOWLEDGMENTS

The authors wish to thank D. E. Holt for helping operate the static pool apparatus and John Cole for operating (and repairing) the DSC. We also thank R. C. DeVault for reviewing and discussing this manuscript.

ABSTRACT

The effectiveness and stability of potential heat-and-mass transfer (performance) additives for an advanced lithium bromide (LiBr) chiller were evaluated in a series of experimental studies. These studies of additive effectiveness and stability were necessary because many currently used performance additives decompose at the high generator temperatures (220°C to 260°C) desired for this particular advanced LiBr chiller. For example, one common performance additive, 2-ethyl-1-hexanol (2EH), reacts with the corrosion inhibitor, lithium chromate (Li_2CrO_4), even at moderate generator temperatures (≥180°C).

These stability problems can be mitigated by using less reactive corrosion inhibitors such as lithium molybdate (Li_2MoO_4) and by using more stable performance additives such as 1-heptanol (HEP) or 1H,1H,7H-dodecafluoro-1-heptanol (DFH). There seems to be a trade-off between additive stability and effectiveness: the most effective performance additives are not the most stable additives. These studies indicate that HEP or DFH may be effective additives in the advanced LiBr chiller if Li_2MoO_4 is used as a corrosion inhibitor.

NOMENCLATURE

This section includes a summary and brief description of the symbols used in this report. More detailed descriptions are provided at the appropriate locations in the text.

Symbol	Definition/Description
E	Mass Transfer Enhancement. Mass ratio of water vapor absorbed with additive to water vapor absorbed without additive in static pool experiments.
E_M	Maximum Mass Transfer Enhancement. Maximum value of E for a particular performance additive in static pool experiments.
E_H	Heat Transfer Enhancement. Ratio of absorber heat transfer coefficient with additive to heat transfer coefficient without additive in minisorber experiments.
$\overline{E}_H$	Average Heat Transfer Enhancement. Average value of E_H at additive concentrations above the threshold necessary for maximum enhancement in the minisorber experiments.
[LiBr]	Lithium Bromide (LiBr) Concentration. Concentration of LiBr in absorber solution in either static pool or minisorber experiments (wt %).
$\dot{m}$	Solution Mass Flow Rate. Mass flow rate of the LiBr solution entering absorber in minisorber experiments (g/min).
T	LiBr Solution Temperature. LiBr solution temperature in static pool experiments (°C).
T_F	Average Solution Film Temperature. Average film temperature of the LiBr film on absorber tube in minisorber experiments (°C).
T_R	Additive Reaction Onset Temperature. Temperature at which additive begins to react or decompose in the differential scanning calorimeter (°C).
X	Performance Additive, X. Identity of the performance additive, X, in the LiBr solutions in the static pool or minisorber experiments.
[X]	Additive Concentration. Concentration of additive, X, in the LiBr solution in either static pool or minisorber experiments (weight parts per million, wppm).

$[X]_M$ Optimum Additive Concentration for Maximum Enhancement. Additive concentration in LiBr solution at which performance enhancement, E, is a maximum in static pool experiments (wppm).

1. INTRODUCTION

Conventional single- and double-effect absorption chillers operate at generator temperatures below 170°C with lithium bromide (LiBr) and water as the absorbent solution.[1] They employ a performance additive such as 2-ethyl-1-hexanol (2EH) to enhance heat and mass transfer and a corrosion inhibitor such as lithium chromate (Li_2CrO_4) to protect the chiller components. The aqueous LiBr solution may also be buffered with a small amount of lithium hydroxide (LiOH) to optimize corrosion inhibition.[2]

Several advanced chiller cycles have been identified that show technical and economic potential. The advanced cycles under consideration are for triple-effect class chillers that can potentially operate at 50% higher efficiency than the best currently used double-effect equipment.[3] Most of the advanced cycles require component operation at temperatures significantly higher than those of present equipment.

The advanced LiBr chiller cycle of immediate interest requires generator temperatures between 220° and 260°C.[4] Several issues arise because of the higher generator temperature. These technical issues were discussed in detail in a previous document.[5] Briefly, these issues include (1) additive effectiveness, (2) additive thermal stability, (3) additive reactivity with corrosion inhibitors (chemical stability), and (4) corrosion resistance of generator materials. The additive effectiveness and stability issues may present major technical problems to LiBr chiller development because there is insufficient understanding of (1) how performance additives work, (2) the thermal stability of current additives, and (3) interactions between additives and corrosion inhibitors.

This report describes experimental studies of performance additive effectiveness and stability. Three experimental activities were undertaken to evaluate potential additives: (1) static performance screening of a large selection of candidates, (2) subsequent dynamic performance testing of a few of the best candidates, and (3) subsequent stability testing of these performance additives at conditions relevant to advanced LiBr chiller operation. The experimental procedures and equipment used in these studies are described in Section 2 of this report. In Section 3, results of these experimental studies are presented. The implications of these results are then discussed in Section 4 and summarized in Section 5 of this report.

2. EXPERIMENTAL PROCEDURE AND DESCRIPTION

2.1 Static Performance Screening

A large number of performance additive candidates were screened by measuring their effects on the rate of water vapor absorption in a static pool of aqueous LiBr. Such static pool absorption tests have previously been used by several researchers to estimate the effectiveness of performance additives.[6,7] Static pool tests are cheaper and faster than dynamic tests and provide an easy method of screening performance additives. However, because static pool conditions are different than those encountered in a falling film absorber, static pool tests cannot quantitatively predict additive performance in an operating chiller.

The experimental equipment used in these studies is similar to that described by other researchers.[7,8] A typical static pool measurement consisted of exposing a 50-ml sample of 60 wt % aqueous LiBr at 20°C to a constant pressure of water vapor (≈17.5 torr). The LiBr solution and water vapor reservoir were contained in a vacuum system to facilitate water vapor absorption at subatmospheric pressures. The surface area of LiBr solution exposed to water vapor was ~63 cm^2.

Static screening exposures were conducted in the following manner. Prior to each exposure, the water vapor reservoir and LiBr solution were degassed at low pressure to remove noncondensible gases such as nitrogen or oxygen. During each exposure, the LiBr solution temperature slowly increased as water vapor was adiabatically absorbed for 15 minutes. After each exposure, the quantity of absorbed water vapor was determined from the change in LiBr concentration by measuring the refractive index of the LiBr solution. In a typical experiment, between 2 and 7 g of water vapor was absorbed by the LiBr solution during a 15-minute exposure. The relative enhancement of a specific performance additive was determined by comparing the quantity of absorbed water vapor in experiments with and without the additive. The relative enhancement was then determined as a function of additive concentration for each additive evaluated.

2.2 Dynamic Performance Testing

Although static pool tests are cheaper and faster than dynamic falling-film absorber tests, static pool tests cannot predict machine performance because test conditions are different. For example, brine exposure time, film thickness, film hydrodynamics, and temperature gradients are significantly different in a static pool than in a falling film absorber.[9] Dynamic minisorber (or single-tube absorber) tests are necessary to quantitatively measure heat-and-mass transfer enhancement because the static pool conditions are not comparable to machine absorber operation.

Several of the most promising additives evaluated in the static pool were subsequently tested in a falling film minisorber. The experimental design of this minisorber has previously been described in some detail.[10] A schematic of the minisorber is shown in Figure 1. Briefly, the falling film absorber consists of a single vertical tube, 19 mm in diameter and approximately 1 m in length. Instrumentation on the minisorber was automated to continuously measure LiBr solution flow rates and temperatures. These temperatures and flow measurements were used to calculate absorber heat transfer coefficients. Mass transfer coefficients could not be accurately determined because of instrument limitations.

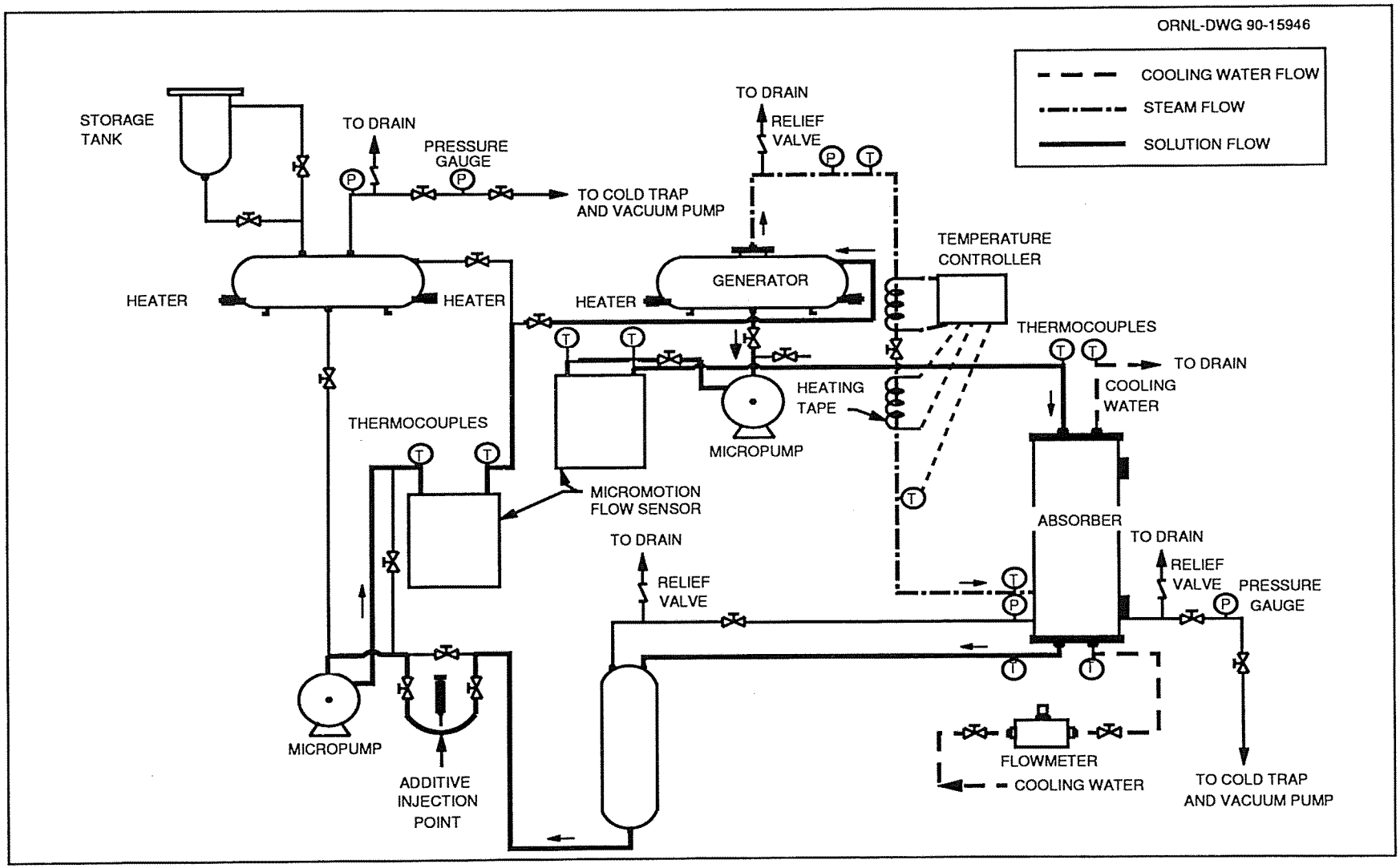

Fig. 1. Schematic of minisorber apparatus used to evaluate performance additive effectiveness.

During a typical minisorber experiment, the solution concentration entering the absorber was 61 wt % LiBr, while the solution concentration leaving the absorber was ~57 wt % LiBr. The average solution film temperature in the absorber was maintained between 92°C and 96°C. (Lower film temperatures could not be attained due to previous minisorber design constraints.[10]) Performance additive effectiveness was determined by comparing steady-state absorber heat transfer with and without an additive present. For each additive evaluated in the minisorber, effectiveness was determined at several different additive concentrations.

2.3 Stability Measurements

Stability testing is necessary to determine the extent of additive decomposition at high generator temperatures (220°C to 260°C). Previous results indicated that at high temperatures additives can either thermally decompose[11] or can react with corrosion inhibitors.[2] Initially, we planned to evaluate additive stability at conditions (temperatures, concentrations, and pressures) anticipated in the high-temperature generator. However, because performance additives and corrosion inhibitors are typically present in very dilute concentration (~100 wppm to 2000 wppm), it was not possible to accurately measure additive stability at these conditions. (Accurate measurements required quantitative extraction of trace amounts of additive from the LiBr solution. Attempts to perform this extraction were not quantitative and not reproducible.[12]) Instead, relative rates of additive decomposition and additive reaction with corrosion inhibitors were determined as functions of temperature using a differential scanning calorimeter (DSC).

The DSC measures the enthalpy changes produced by thermal decomposition or chemical reaction. When a sample in the DSC is heated at a constant rate, its temperature increases linearly with time. The DSC is purged and backfilled with argon to prevent sample reaction with ambient oxygen during heating. Sample decomposition or reaction is indicated by a change in the quantity of heat flowing into the sealed sample capsules. The temperature at which the change in heat flow occurs (onset temperature) is an indicator of relative sample stability. The higher the onset temperature, the more stable the sample.

The relative thermal and chemical stabilities of several additives were compared using the DSC. Thermal stability was evaluated by measuring the onset temperature for each additive. Relative thermal stability of the additives was determined by comparing onset temperatures. Chemical stability of various additives was evaluated in a similar manner. The onset temperatures of specific additive-inhibitor mixtures were measured in the DSC to determine the chemical stability of each mixture. Two corrosion inhibitors commonly used in LiBr chillers are Li_2CrO_4 and lithium molybdate (Li_2MoO_4). In these studies, potassium chromate (K_2CrO_4) was substituted for Li_2CrO_4, and sodium molybdate (Na_2MoO_4) was substituted for Li_2MoO_4 as an experiment convenience. (The substituted chemicals were readily available; the lithium compounds were not. Chemical reactivity of performance additives with the substituted inhibitors should be essentially identical to additive reactivity with the lithium inhibitors.) Comparison of mixture onset temperatures provided a relative measure of the chemical stability of various additive-inhibitor combinations.

3. RESULTS

3.1 Static Performance Enhancement Results

The performance enhancement of various additives was determined by comparing the mass of water vapor absorbed by LiBr solutions with and without additive present. To facilitate this comparison, a mass transfer enhancement, E, was defined. Enhancement, E, is the mass of water absorbed in an LiBr solution containing additive, divided by mass of water absorbed in a similar LiBr solution not containing any additive. The performance enhancement measurements, E, for various concentrations of 2EH, [2EH], are summarized in Table 1. These results were obtained in aqueous LiBr solutions where, initially, T = 20°C and [LiBr] = 60 wt %.

Table 1. Performance (mass transfer) enhancement, E, as a function of 2-ethyl-1-hexanol concentration, [2EH][a,b]

[2EH] (wppm)	E
0	1.0
210	4.9
315	5.3
415	6.4
625	8.3
680	7.5
780	7.6
990	3.5
1380	1.8

[a]Initial Conditions: [LiBr] = 60 wt %, T = 20°C.
[b]E_M = 9.0, $[2EH]_M$ = 566 wppm.

The performance enhancements in Table 1 are strongly dependent on [2EH]. As 2EH is added to the LiBr solution, E initially increases with [2EH] until E reaches a maximum value, E_M, where [2EH] = $[2EH]_M$. Further addition of 2EH decreases E. The variation in enhancement with concentration is shown in Figure 2, where E is displayed as a function of [2EH]. The open circles in this figure are the experimental results from Table 1. The experimental results in Figure 2 were used to estimate E_M and $[2EH]_M$ using a straightforward (but theoretically unjustified) empirical interpolation. For [2EH] < 416 wppm, E increased with increasing [2EH], indicating that $[2EH]_M$ > 416 wppm. This increase in E with [2EH] was represented by the line segment in Figure 2 having the positive slope.

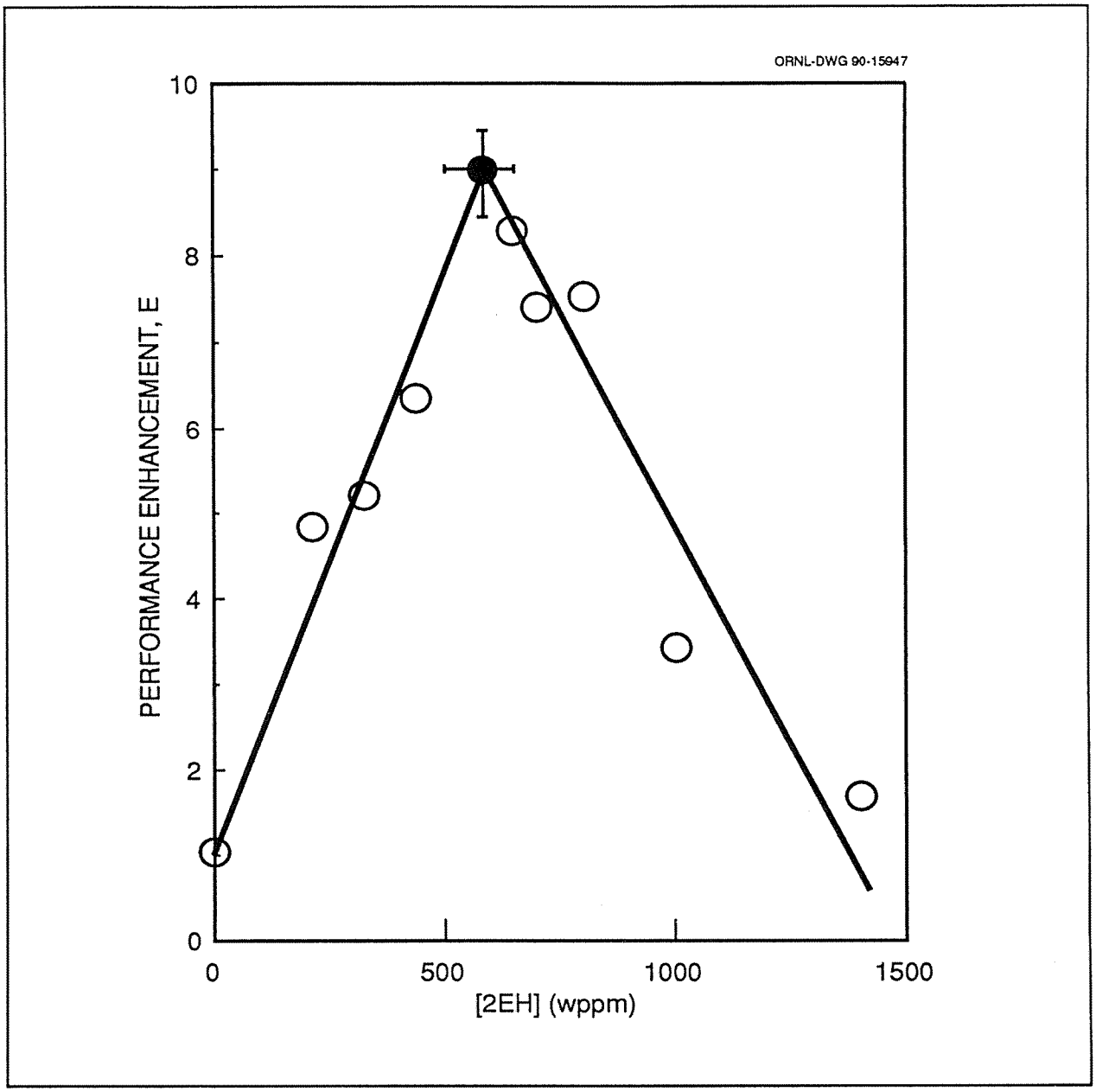

Fig. 2. Performance (mass transfer) enhancement, E, as a function of 2-ethyl-1-hexanol concentration, [2EH], in a static pool of aqueous LiBr. The open circles are experimental measurements of performance enhancement, while the solid lines are empirical representations of the data. The solid circle is an estimate of the maximum performance enhancement, E_M. The error bars indicate the uncertainties in E_M and $[2EH]_M$.

For [2EH] > 625 wppm, E decreased with increasing [2EH], indicating that $[2EH]_M$ < 625 wppm. This decrease in E is represented by the line segment in Figure 2 having the negative slope. The two line segments intersected at the solid circle, which is the empirical

estimate of E_M and $[2EH]_M$. In Figure 2, E_M = 9.0 and $[2EH]_M$ = 565 wppm, within the uncertainties indicated by the error bars.

Similar static pool enhancement measurements were conducted using 1-heptanol (HEP), 1H,1H,7H-dodecafluoro-1-heptanol (DFH), and 1,1,1-trifluoro-2-octanol (TFO) as performance additives. These results are summarized in Tables 2–4, respectively. The performance enhancements obtained with HEP, DFH, and TFO also show a strong dependence on additive concentration. As with 2EH, performance enhancement reaches a maximum value, E_M, at some optimum additive concentration. Estimates of E_M and optimum additive concentrations are indicated in Tables 2–4 for the respective additives. These values were obtained using the same interpolation procedure illustrated in Figure 2.

Table 2. Static performance enhancement, E, as a function of 1-heptanol concentration, [HEP][a,b]

[HEP] (wppm)	E
0	1.0
205	4.6
410	7.5
580	6.8
680	7.9
680	7.9
680	6.5
825	4.8

[a]Initial Conditions: [LiBr] = 60 wt %, T = 20°C.
[b]E_M = 8.8, $[HEP]_M$ = 600 wppm.

Table 3. Static performance enhancement, E, as a function of 1H,1H,7H-dodecafluoro-1-heptanol concentration, [DFH][a,b]

[DFH] (wppm)	E
0	1.0
225	2.5
445	3.3
880	4.4
1326	2.0
1760	0.4
2640	0.5

[a]Initial Conditions: [LiBr] = 60 wt %, T = 20°C.
[b]E_M = 5.0, $[DFM]_M$ = 730 wppm.

Table 4. Static performance enhancement, E, as a function of 1,1,1-trifluoro-2-octanol concentration, [TFO][a,b]

[TFO] (wppm)	E
0	1.0
260	1.8
515	2.6
645	2.8
775	2.0
1030	2.0

[a]Initial Conditions: [LiBr] = 60 wt %, T = 20°C.
[b]E_M = 2.9, $[TFO]_M$ = 590 wppm.

The enhancement dependence on additive concentration observed in Figure 2 for 2EH and in Tables 2 through 4 for HEP, DFH, and TFO was also observed for the other additives. For each additive tested in the static pool, E initially increased with additive concentration, X, until a maximum enhancement, E_M, was obtained at an optimum additive concentration, $[X]_M$. For $[X] > [X]_M$, E decreased with increasing [X]. Each additive, X, evaluated in the static pool tests could be characterized by $[X]_M$ and by E_M. The results of all screening studies (including those previously described in Tables 1 through 4) are summarized in Table 5. For the 12 additives, X, listed in column 1 of Table 5, the optimum additive concentration, $[X]_M$, is listed in column 2. The maximum performance enhancement, E_M, is listed in column 3. Most of the additives listed in this table were only slightly soluble in aqueous LiBr (solubility ~100–800 wppm). The exceptions are noted in Table 5.

The values of E_M in Table 5 vary from 1.6 to 9.1. For the most effective additives ($E_M >$ 6), water vapor absorption was accompanied by agitation of the LiBr solution at the liquid/vapor interface. (Interfacial agitation was not observed in experiments with LiBr solutions not containing additives.) This additive-induced agitation has been observed by many other researchers.[6,7] It has generally been attributed to Marangoni convection. (See Section 4 for alternate explanations of the additive enhancement mechanism.) This "Marangoni" agitation presumably increases the water absorption rate by helping mix LiBr solution near the liquid/vapor interface with LiBr solution far from the interface.[13]

Several experiments were performed to compare Marangoni agitation (due to performance additives) with mechanical agitation produced by stirring (using a magnetic "stirring bar"). The results of these experiments are summarized in Table 6. Mechanical agitation alone produced slightly less enhancement (E_M = 8.1) than did the performance additive, 2EH (E_M = 9.0). The combination of mechanical agitation and a performance additive produced slightly more enhancement (E_M = 9.3) than did 2EH alone (E_M = 9.0).

Table 5. Maximum static enhancement, E_M, of various additives

ADDITIVE, X	$[X]_M$ (wppm)	E_M
2-Ethyl-1-hexanol	565	9.0
1-Heptanol	600	8.8
1H,1H,7H-Dodecafluoro-1-heptanol	730	5.0
1,1,1-Trifluoro-2-octanol	590	2.9
1-Octanol	680	8.4
2-Octanol	580	7.9
3-Octanol	600	9.1
1-Decanol	680	7.4
1-Octene-3-ol	520	8.1
2,6-Dimethyl-4-heptanol	610	5.0
2-Methyl-2-propanol[S]	3500	5.5
1,2-Hexanediol	780	2.8
1,6-Hexanediol	920	3.1
2-Heptenal	604	5.0
15-Crown-5	850	2.9
Surfactant FC450[S]	790	2.8
Surfactant FC135[S]	820	1.9
Surfactant FC99[S]	760	1.6

[S]Soluble in $LiBr/H_2O$ solution

Table 6. Comparison of performance enhancement, E_M, with mechanical stirring and performance additives.

ADDITIVE	STIRRING	E_M
2EH	Yes	9.3
2EH	No	9.0
None	Yes	8.1
None	No	1.0

The slight synergism between Marangoni agitation and mechanical agitation shown in Table 6 prompted the investigation of potential synergism between additives. The observed

changes in performance when a second additive is combined with 2EH are summarized in Table 7. The results in this table indicate that essentially no changes in performance occur when either HEP or DFH are combined with 2EH. However, when 2-methyl-2-propanol (2MP) is combined with 2EH, a 10% increase in performance occurs. Although the reason for the synergism between 2EH and 2MP is unknown, it may be that 2MP behaves differently from most other additives. Unlike the other additives in Table 7 and most of the effective additives evaluated in this study, 2MP is very soluble in aqueous LiBr, and 2MP does not produce visible Marangoni convection.

Table 7. Effect of additive combination on performance enhancement

ADDITIVE 1	ADDITIVE 2	E_M
2EH	None	9.0
2EH	HEP	8.8
2EH	DFH	9.0
2EH	2MP	9.9

3.2 Dynamic Performance Enhancement Results

The static screening results led to the selection of (1) four additives: 2EH, HEP, DFH, and TFO and (2) a mixture of 2EH and 2MP for further testing in dynamic performance experiments. The additives chosen for further testing embodied some of the most desirable characteristics of all additives tested in the static pool. Two additives, 2EH and HEP, were selected for dynamic testing because of their excellent performance enhancement. Two other additives, DFH and TFO, were selected because of their (predicted) superior thermal and chemical stability.[14] The mixture of 2EH and 2MP was evaluated because of the enhancement synergism observed in Table 7.

Each additive and additive mixture was evaluated for a range of concentrations in the minisorber using the experimental procedure described in the previous section. Dynamic performance enhancement was determined by comparing absorber heat transfer with and without additive. Results from a typical minisorber experiment are shown in Figure 3. In this figure, the enhancement ratio, E_H (which is the ratio of the heat transfer coefficient with additive to the heat transfer coefficient without additive), is shown as a function of [2EH]. The circles are experimental results obtained at an absorber film temperature, T_F = 92°C, with an LiBr solution flow rate, $\dot{m}$ = 603 g/min. Initially, E_H = 1 with no additive present (by definition), then increased to a maximum value as [2EH] increased. Unlike the static pool measurements, further increases in [2EH] did not change E_H. Within experimental

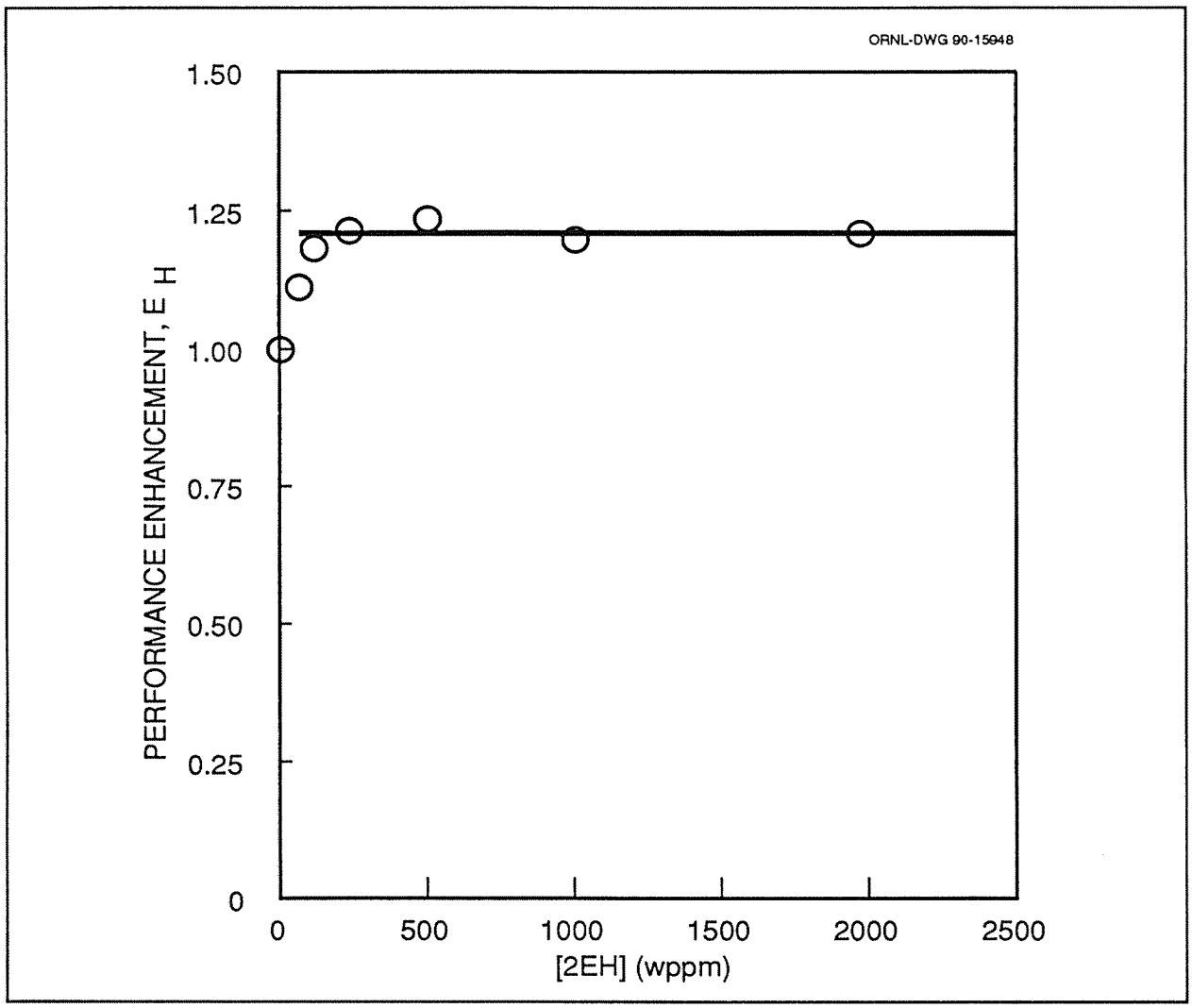

Fig. 3. Performance (heat transfer) enhancement, E_H, as a function of 2-ethyl-1-hexanol concentration, [2EH], in a falling film absorber. The circles are experimental results obtained at T_F = 92°C and $\dot{m}$ = 603 g/min. The solid line is the average performance enhancement, $\overline{E}_H$.

uncertainty, E_H remained constant above a threshold [2EH]. Above the threshold [2EH], the average performance enhancement, $\overline{E}_H$, was $\overline{E}_H = 1.19 \pm 0.01$ as indicated by the solid horizontal line in Figure 3.

The enhancement results in Figure 3 were typical of the behavior observed in minisorber experiments for other effective performance additives. The average dynamic enhancement, $\overline{E}_H$, was relatively independent of [X] for additive concentrations above a threshold value. (This insensitivity to additive concentration is consistent with other falling film enhancement studies.[9]) However, $\overline{E}_H$ did vary slightly with T_F and significantly with $\dot{m}$. Therefore, in order to compare the performance enhancement of different additives, $\overline{E}_H$ was evaluated for similar T_F and $\dot{m}$. The results of the dynamic performance evaluations are summarized in Table 8. Qualitatively similar results were obtained at other mass flow rates. The results in this table indicate that only 2EH, HEP, and DFH showed sufficient enhancement ($E_H > 1$) to warrant further evaluation.

Table 8. Minisorber performance enhancement of various additives[a]

ADDITIVE(S)	$\overline{E}_H$
2EH	1.19 ± .01
HEP	1.25 ± .04
DFH	1.07 ± .01
TFO	0.95 ± .03[b]
2EH & 2MP	0.74 ± .05[c]

[a]Absorber operating conditions at T = 96°C and $\dot{m}$ = 605 g/min.
[b]E_H decreased with increasing [TFO].
[c]E_H decreased with increasing [2MP].

3.3 Thermal and Chemical Stability Results

Only 2EH, HEP, and DFH were deemed sufficiently effective (Table 8) to justify the evaluation of their thermal and chemical stability. The relative thermal stability of these additives was evaluated by determining onset temperatures, T_R, using the DSC. A typical thermal stability evaluation is shown in Figure 4. In this figure, the heat flowing into a 2EH sample is shown as a function of the sample temperature as the DSC is slowly heated at a constant rate (10°C/min). The peak at 224°C is due to heat generated from the thermal decomposition of 2EH. The arrow at T_R = 207°C indicates the onset of thermal decomposition for 2EH. The relative thermal stability of HEP and DFH were determined in a similar manner.

The relative chemical stability of a particular additive depends on the other chemicals—primarily the corrosion inhibitor—present in the absorber fluid.[2] An initial estimate of chemical stability was determined for specific additive/inhibitor mixtures. Each additive was mixed with a sufficient amount of corrosion inhibitor (either chromate or molybdate) to oxidize each additive to yield the corresponding carboxylic acid.[15] (This computation was used only to compare similar molar quantities of the various performance

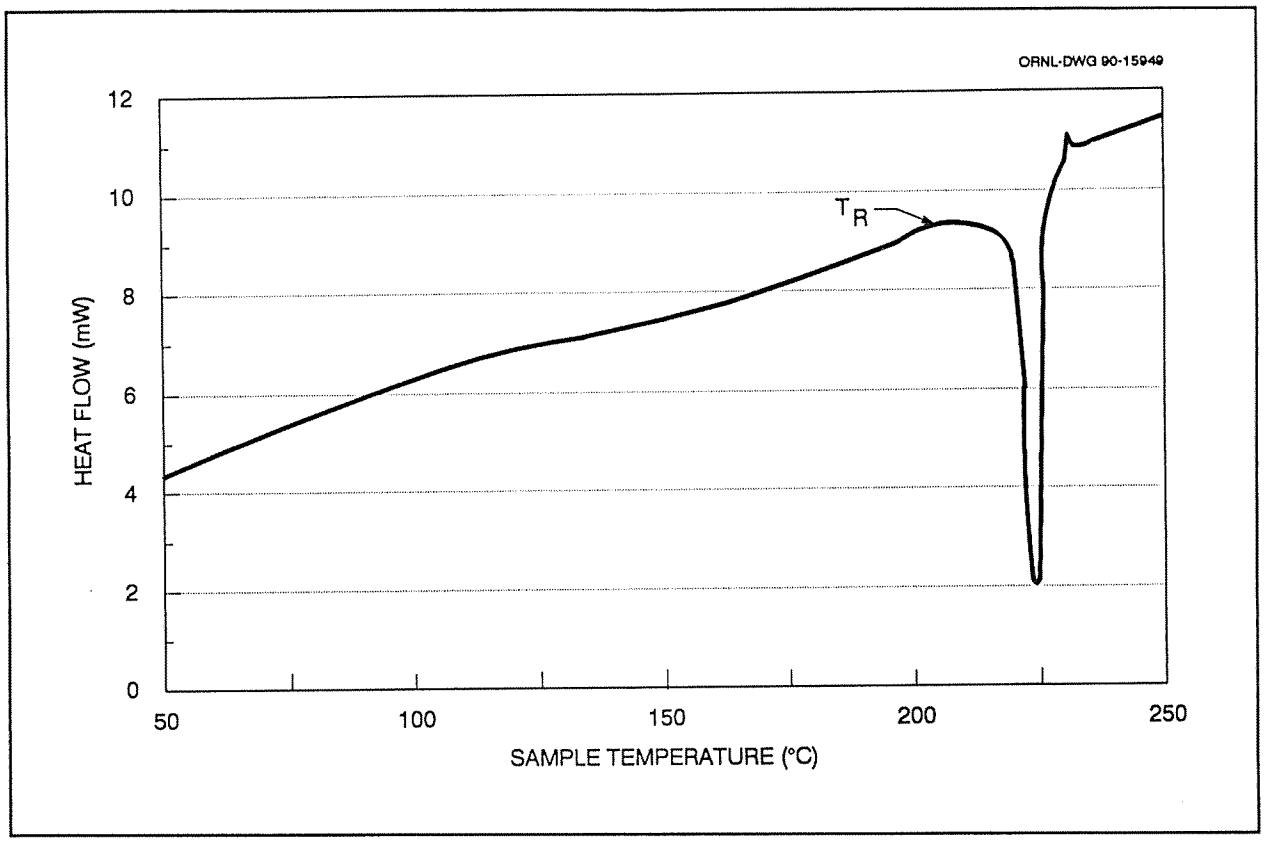

Fig. 4. Thermal stability of 2EH (2-ethyl-1-hexanol) obtained by DSC (differential scanning calorimetry). The heat flow rate into a 2EH sample is shown as a function of temperature as the DSC is slowly heated (at 10°C/min). The peak at 225°C indicates a sample enthalpy change due to thermal decomposition. The arrow at T_R = 207°C indicates the onset of thermal decomposition.

additives and corrosion inhibitors. No assumptions about the nature or stoichiometry of the reactions involved were made).

A typical DSC for one specific additive/inhibitor mixture is shown in Figure 5. In this figure, heat flowing into a mixture of HEP and K_2CrO_4 is shown as a function of DSC temperature. The peak at 218°C is due to HEP's reaction with K_2CrO_4. The arrow at T_R = 210°C indicates the onset of HEP's reaction with Li_2CrO_4. The relative chemical stabilities of the other additives with chromate and molybdate were determined in a similar manner.

The results of thermal and chemical stability evaluations of these three additives are summarized in Table 9. For the test conditions indicated in column 1, T_R is listed for 2EH, HEP, and DFH in columns 2–4, respectively. The test conditions evaluated include additive alone (for an indication of thermal stability), additive/inhibitor mixtures (for a preliminary indication of chemical stability), and additive/inhibitor mixtures in an aqueous LiBr solution (to more closely simulate the actual chemical environment expected during generator operation). Table 9 indicates that, as expected, the stability of DFH is much better than that of either HEP or 2EH. The stability of HEP is also slightly better than that of 2EH. At the test conditions listed in the last row of Table 9, T_R for HEP is 11°C greater than T_R for 2EH.

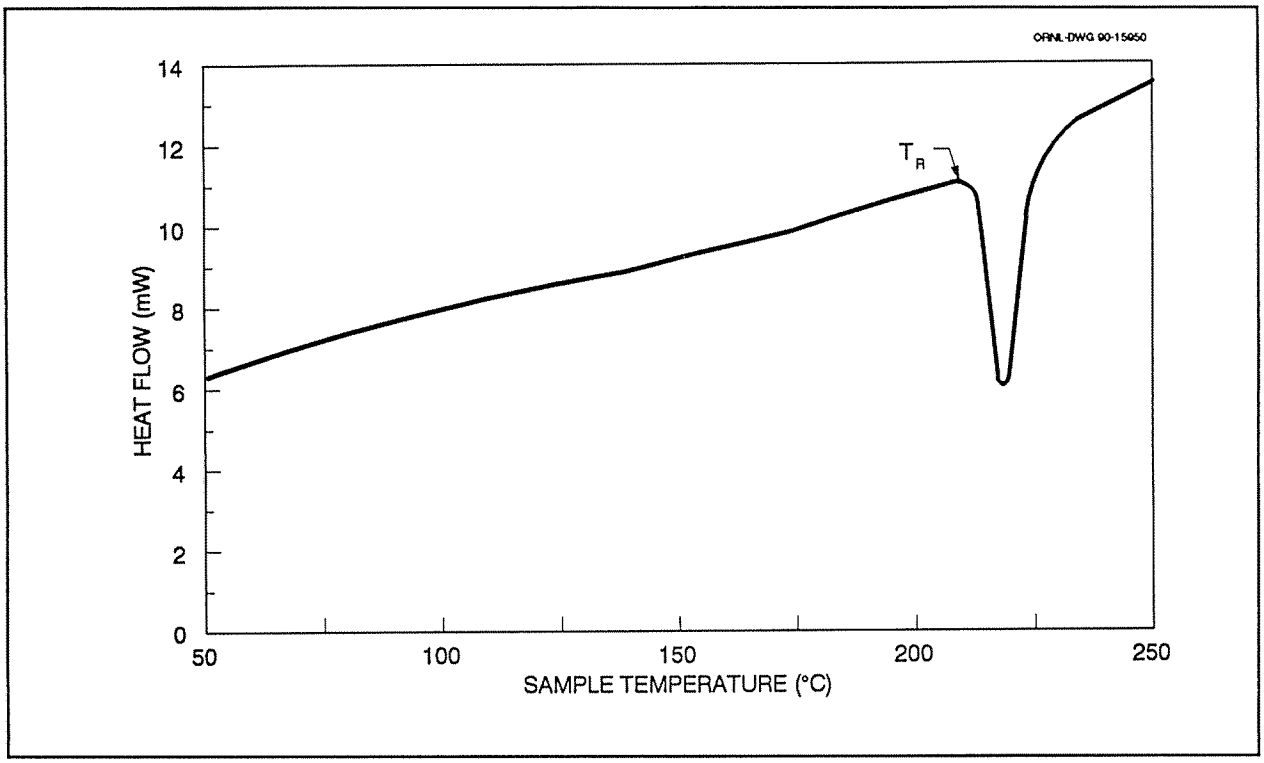

Fig. 5. Chemical stability of 1-heptanol(HEP)-chromate mixture obtained by DSC (differential scanning calorimetry). The heat flow into a mixture of HEP and K_2CrO_4 is shown as a function of sample temperature as the DSC is slowly heated (at 10°C/min). The peak at 218°C indicates a mixture enthalpy change caused by reaction. The arrow at T_R = 210°C indicates the onset of chemical reaction.

Table 9. Stability of performance additives in various environments

TEST CONDITIONS	ADDITIVE REACTION ONSET TEMPERATURE, T_R (°C)		
	2EH	HEP	DFH
Additive only	207	216	>300
Additive + K_2CrO_4	198	210	>300
Additive + Na_2MoO_4	200	203	>300
Additive + K_2CrO_4 + (H_2O + LiBr)[a]	249	>245[b]	--
Additive + Na_2MoO_4 + (H_2O + LiBr)[a]	230[c]	241	--

[a]60 wt % LiBr, 0.1 wt % LiOH in H_2O; LiBr solution is 45% of total sample weight.
[b]Experiment terminated to limit H_2O pressure in sample capsule.
[c]LiBr solution is 25% of total sample weight.

These test conditions more closely simulate the chemical environment anticipated during generator operation in the advanced chiller because the additive and corrosion inhibitors have been diluted with LiBr solution. (The alkalinity was also adjusted to closely represent alkalinity anticipated in generator operation.[2]) However, even at these conditions, the corrosion inhibitor concentrations in Table 9 are 200 to 2000 times greater than anticipated in the high temperature generator.

As indicated in rows 4 and 5 of Table 9, after aqueous LiBr solutions were added to specific additive/inhibitor mixtures, reaction onset temperatures increased 30°C to 40°C. The increases in T_R for a particular additive/inhibitor were approximately proportional to the quantity of added LiBr solution, indicating that the LiBr solution was acting as an inert diluent. As expected, the additive's reaction with a corrosion inhibitor depends on the concentration of corrosion inhibitor in the LiBr solution.

Unfortunately, because of experimental difficulties it was not possible to evaluate the dependence of T_R on corrosion inhibitor concentration at more realistic conditions. When LiBr solutions were added to the DSC sample capsules, the vapor pressure of water exceeded the capsule pressure limit at temperatures above 240°C. When this limit was exceeded, the capsules would occasionally rupture and contaminate the DSC. Because of this problem, the higher onset temperatures of more dilute solutions (which would be more representative of actual generator conditions) could not be studied.

4. DISCUSSION

4.1 Static Performance Enhancement

Determining the mechanism(s) responsible for performance enhancement is difficult because of the apparent complexity of the interactions and the dearth of definitive experimental results. Different mechanisms describing the role of additives in heat and mass transfer have been proposed. Several studies attribute the performance enhancement to agitation of the solution at the vapor interface produced by Marangoni convection.[6–9] A catalytic mechanism, by which the activation energy of absorption is reduced by the additive, has also been proposed.[16] Other explanations for the performance enhancement postulate that additives may clean the heat exchanger surface or that additives may promote dropwise condensation.[5]

Although several mechanisms have been proposed to explain how additives enhance heat and mass transfer, the results in this study seem most consistent with Marangoni-induced convection in the static pool. For almost all of the effective additives evaluated in Table 5, performance enhancement was strongly correlated with agitation of the LiBr solution surface. The more surface agitation, the more performance enhancement. The mechanical stirring results in Table 6 also seem consistent with Marangoni-induced agitation. The maximum enhancement produced by mechanical stirring is only slightly smaller than the enhancement produced by the performance additive 2EH. The enhancement produced by a combination of additive and mechanical stirring is also not significantly better than that produced by 2EH alone. The results in Table 6 suggest that most of the enhancement (~90%) from 2EH is due to agitation of the LiBr solution.

The behavior of most of the effective additives evaluated in this study was similar to that of 2EH. One additive which behaved differently was 2MP. In static pool experiments, 2MP enhanced performance but did not produce surface agitation. As indicated in Table 7, 2MP was also the only additive which had a synergistic effect when coupled with 2EH. Since 2MP is completely soluble in aqueous LiBr, no second phase of 2MP forms at the solution/vapor interface. This second phase is thought to be necessary for Marangoni agitation.[6,17] Perhaps 2MP enhances heat and mass transfer by reducing the activation energy of absorption (as proposed by Biermann).[16] Another possibility is that 2MP changes some fluid transport property, such as viscosity.

4.2 Dynamic Performance Enhancement

Comparison of Tables 5 and 8 indicates general qualitative agreement between static and dynamic enhancement results for the additives evaluated by both methods. (Quantitative agreement is not expected because of differences in testing conditions—film thickness, vapor residence time, fluid velocity, etc.[5]) The additives producing the most static enhancement, 2EH and HEP, also produce the most dynamic enhancement. The additive producing the least static enhancement, TFO, also produced the least dynamic enhancement. The static and dynamic performance enhancement of DFH was intermediate between TFO and HEP.

One significant disparity between static and dynamic results was in the behavior of the 2EH/2MP mixture. In the static tests (summarized in Table 7), this mixture enhanced performance approximately 10% more than did 2EH alone. However, in the dynamic

performance tests (Table 8), addition of 2MP to 2EH decreased heat and mass transfer to $E_H < 1$. One possible explanation for this disparity is the high solution temperature in the minisorber (96°C) relative to that of the static LiBr pool (20°C). Because 2MP boils at 83°C,[18] most of the 2MP added to the LiBr solution in the minisorber probably vaporized. The presence of a high partial pressure of 2MP in the minisorber should inhibit water vapor absorption in the same manner that inert gases inhibit water vapor absorption. If the minisorber could have been operated at a lower temperature, more 2MP would have remained in solution and, perhaps, improved absorber performance.

4.3 Thermal and Chemical Stability

This study was directed toward testing additives structurally similar to 2EH but having slightly greater thermal stability. This experimental approach was justified because previous measurements by other researchers indicated that 2EH had satisfactory thermal and chemical stability at generator temperatures near 220°C.[11] (These previous measurements suggest that 2EH might even be satisfactory at advanced chiller temperatures with some modifications in chiller design.[5] See Section 4.4.) Generally, the thermal stability of aliphatic compounds (1) increases slightly as the number of carbon atoms decreases and (2) increases significantly as fluorine is substituted for hydrogen.[19]

The thermal results in Table 9 agree with these predictions. The thermal stability of HEP (which contains seven carbon atoms) is slightly greater than that of 2EH (which contains eight carbon atoms). The thermal stability of the fluorinated additive, DFH, is significantly greater than that of the unfluorinated additive, HEP. Although the presence of a corrosion inhibitor or LiBr solution changes T_R, the additives in Table 9 have a similar hierarchy in chemical and thermal stability. For a particular corrosion inhibitor, DFH is much more stable than HEP, which is slightly more stable than 2EH.

For 2EH, Table 9 shows that chromate is a slightly more reactive inhibitor than molybdate. In previous studies, differences between chromate and molybdate reactivity were more pronounced. For example, one study showed significant 2EH reaction with Li_2CrO_4 at 180°C,[1] while another study showed only moderate 2EH reactivity with Li_2MoO_4 at 220°C.[11] The apparent discrepancy between Table 9 and the earlier results is due to differences in inhibitor concentration. When Li_2CrO_4 is used as a corrosion inhibitor in LiBr, a typical concentration is 2700 wppm.[1] A typical Li_2MoO_4 concentration in LiBr is 300 wppm.[11] Since reactivity is strongly dependent on concentration,[2] the greater inhibitor concentration (factor of 12 on a molar basis) partially explains the increased chromate reactivity. The remaining difference in reactivity is due to chromate's being a stronger oxidizing agent than molybdate.[20]

The results in Table 9 provide relative stability estimates of various inhibitor/additive combinations. The higher the T_R, the more stable the inhibitor/additive combination. The results in Table 9 can also be combined with previous stability measurements to crudely estimate additive decomposition rates. For example, in a previous stability study, approximately 7% of the 2EH in an LiBr solution containing Li_2MoO_4 decomposed after 168 hours at 227°C.[11] Since HEP in molybdate is slightly more stable than 2EH in molybdate, less additive decomposition would be expected if HEP were evaluated at similar conditions. (At the most representative conditions in Table 9, T_R is ~11°C greater for HEP than for 2EH.) No additive decomposition would occur if DFH were evaluated at these generator conditions.

4.4 Implications for Advanced Chiller Development

Ideally, potential additives for the advanced chiller would have superior performance enhancement as well as superior thermal and chemical stability. Unfortunately, the results in Tables 5 and 8 indicate that a compromise between stability and performance may be required. Table 5 indicates that the performance enhancement of HEP is slightly better than that of 2EH, which is significantly better than that of DFH. However, Table 8 indicates that the stability of DFH is significantly better than that of either HEP or 2EH. If HEP has sufficient stability, it would produce more enhancement than DFH in the advanced chiller. The discussion in the previous paragraph suggests that HEP may be satisfactory at generator temperatures between 220°C and 235°C.

We are unaware of any obvious, fundamental reason for the apparent compromise between additive stability and performance. Perhaps more potential performance additives need to be evaluated. A candidate additive may exist that has both superior performance enhancement and thermal stability.

Some technical problems associated with alcohol decomposition at high temperatures may be overcome by design modifications. At the lower limit of the desired generator temperature (~220°C), HEP may have satisfactory thermal stability if Li_2MoO_4 can be used as a corrosion inhibitor. Higher generator temperatures may be possible if additional additive can be supplied to the absorption solution or if additive can be separated from the absorber solution before the solution enters the generator. Adequate purge capacity would also be required to remove volatile decomposition byproducts. The effects of nonvolatile decomposition products on heat and mass transfer must also be considered. Decomposition products could "poison" the additive enhancement or even coat heat exchanger surfaces. (Fortunately, some previous experiments indicate that this is not often a problem.[17]) Each of these design strategies will be evaluated in the advanced chiller development program.[5]

If, after applying the design modifications described in the previous paragraph, HEP still has insufficient thermal stability, DFH could be used as a performance additive in the advanced chiller. Although DFH has adequate thermal stability, the performance enhancement of DFH is significantly less than that of either HEP or 2EH. Fortunately, the performance enhancement of DFH may also be improved by a different modification of the advanced chiller design. The results in Table 6 show that most of the performance enhancement of 2EH (and presumably, HEP) can be recovered by agitation at the solution/vapor interface. In the static pool experiments, mechanical agitation (stirring) improved heat and mass transfer almost as effectively as did a performance additive. Similar mechanical agitation could be accomplished in the advanced chiller by modifying the heat exchanger surfaces in the absorber. For example, using absorber tubes with noncylindrical cross-sections and adding fins or turbulence promoters to the tube surfaces might increase agitation at the solution/vapor interface. Such modifications have been used successfully to improve heat and mass transfer in another LiBr-water absorber.[21]

5. CONCLUSIONS

The effectiveness and stability of potential performance additives in the advanced LiBr chiller were evaluated in a series of experimental studies. These studies of additive effectiveness and stability were necessary because many current performance additives decompose at the high generator temperatures desired in the advanced LiBr chiller (220°C to 260°C). These stability problems can be mitigated by using less reactive corrosion inhibitors such as Li_2MoO_4 and by using more stable performance additives such as HEP or DFH.

A trade-off seems to exist between additive stability and effectiveness: the most effective performance additives are not the most stable additives. These studies indicate that HEP or DFH may be effective additives in the advanced LiBr chiller if Li_2MoO_4 is used as a corrosion inhibitor—HEP provides the greatest performance enhancement, and DFH provides the best thermal and chemical stability.

Some technical problems associated with alcohol decomposition at high temperature may be overcome by design modifications. Higher generator temperatures may be possible if additional additive can be supplied to the absorption solution or if additive can be separated from the absorber solution before the solution enters the generator. Adequate purge capacity would also be required to remove volatile decomposition byproducts. Effects of nonvolatile decomposition byproducts must also be considered. Each of these design strategies will be evaluated in the advanced chiller development program.

Performance enhancement measurements indicate that enhancement is strongly correlated with solution agitation. Although several mechanisms have been proposed to explain how additives enhance heat and mass transfer, the results seem most consistent with Marangoni-induced convection in the static pool. The most effective performance additives produced the most agitation at the solution/vapor interface. In the static pool experiments, mechanical agitation improved heat and mass transfer almost as effectively as did a performance additive. Similar mechanical agitation could be accomplished in the advanced chiller by modifying the heat exchanger surfaces in the absorber. This design strategy may also be evaluated in the advanced chiller development program.

REFERENCES

1. *Absorption Operation Maintenance*, AM-FND4-772, The Trane Co., LaCrosse, Wisc., 1972.

2. R. H. Krueger, K. F. Dockus, and W. F. Rush, "Lithium chromate: Corrosion inhibitor for lithium bromide absorption refrigeration systems," *ASHRAE Journal* **6**, 40–44 (1964).

3. R. C. DeVault, "Triple Effect Absorption Chiller Utilizing Two Refrigeration Circuits," U.S. patent 4,732,008, March 1988.

4. "Development and Proof-Testing of Basic Technology Needed for High Temperature Operation of LiBr/H_2O for Absorption Chiller Cycles," Request for Proposal No. SF416-87, Martin Marietta Energy Systems, Inc., May 24, 1990.

5. F. A. Creswick and R. H. Reiner, *Absorber Research Plan for Water-Based Refrigerant Systems*, ORNL/CF-90/342, Oak Ridge Natl. Lab., Martin Marietta Energy Systems, Inc., August 10, 1990.

6. T. Kashiwagi, "Basic Mechanism of Absorption Heat and Mass Transfer Enhancement by the Marangoni Effect," presented at the Advanced Absorption Workshop, Knoxville, Tenn., Oct. 4, 1988.

7. Y. Elkassabgi and H. Perez-Blanco, "Experimental Study of the Effects of Alcohol Additives in Lithium Bromide Water Pool Absorbers," to be presented at ASHRAE Summer Meeting, June 1991.

8. T. Zawacki, S. Leipziger, and S. A. Weil, "Inducement of Convective Motion in Static Absorbers," presented at Fourth Joint Chemical Engineering Conference, Vancouver, B.C., September 1973.

9. T. Kashiwagi, et al., "Marangoni Effect in the Process of Steam Absorption into the Falling Film of the Aqueous Solution of LiBr," presented at the Advanced Absorption Workshop, Knoxville, Tenn., Oct. 4, 1988.

10. A. Zaltash, M. R. Ally, and R. L. Linkous, *Summary of the Experiments and Results to Evaluate the Effects of Additives on LiBr Solutions*, ORNL/CF-90/369, Oak Ridge National Laboratory, Martin Marietta Energy Systems, Inc., December 1990.

11. "Development and Proof-Testing of Advanced Absorption Refrigeration Cycle Concepts - II," Task Report R87-852258-1, Carrier Corporation, November 1987, p. 26.

12. B. A. Tompkins, Analytical Chemistry Division, Oak Ridge National Laboratory, "Progress on Test Plan for Heat Transfer Additive Stability Study," letter to R. H. Reiner, Energy Division, Oak Ridge Natl. Lab., August 29, 1990.

13. G. Grossman, "Heat and Mass Transfer in Film Absorption," pp. 219–223 in *Handbook of Heat and Mass Transfer*, ed. N. T. Cheremisinoss, Gulf Publishing Co., Houston, Tex., 1986.

14. R. Modahl and P. J. Lynch, "Absorption Heat Exchange Systems, Methods and Absorbent Compositions," U.S. patent 3,783,631, January 1974.

15. R. T. Morrison and R. N. Boyd, *Organic Chemistry*, Allyn and Bacon, Boston, 1966, pp. 533–536.

16. W. J. Biermann, *Additives for Enhancing Heat/Mass Transfer in Absorbers*, Oak Ridge Natl. Lab., Martin Marietta Energy Systems, Inc., unpublished data, July 1984.

17. R. Modahl, Trane Corporation, personal communication to R. H. Reiner, Oak Ridge National Laboratory, July 1990.

18. R. T. Morrison and R. N. Boyd, *Organic Chemistry*, Allyn and Bacon, Boston, 1966, p. 501.

19. R. T. Morrison and R. N. Boyd, *Organic Chemistry*, Allyn and Bacon, Boston, 1966, pp. 461–492.

20. H. M. Uhlig, *Corrosion and Corrosion Control*, J. Wiley, New York, 1963, pp. 224–232.

21. R. L. Webb and L. J. Mougin, "Apparatus for Absorbing a Vapor in a Liquid and Absorption Refrigeration System Incorporating Same," U.S. patent 4,223,539, June 1978.

INTERNAL DISTRIBUTION

1. M. R. Ally
2. V. D. Baxter
3. R. S. Carlsmith
4. F. C. Chen
5. G. E. Courville
6. F. A. Creswick
7. R. C. DeVault
8. P. D. Fairchild
9. S. K. Fischer
10. W. Fulkerson
11. P. S. Gillis
12. M. A. Hensley
13. P. J. Hughes
14. M. A. Kuliasha
15. W. P. Levins
16. V. C. Mei
17. W. A. Miller
18. W. R. Mixon
19. R. W. Murphy
20. D. E. Reichle

21-45. R. H. Reiner

46. C. K. Rice
47. M. W. Rosenthal
48. J. R. Sand
49. R. B. Shelton
50. J. A. Shonder
51. J. N. Stone
52. E. A. Vineyard
53. A. Zaltash

54-55. Laboratory Records Department

56. Laboratory Records-RC
57. ORNL Patent Office
58. Central Research Library
59. Document Reference Section

EXTERNAL DISTRIBUTION

60. D. A. Ball, Battelle Columbus Laboratories, 505 King Avenue, Columbus, OH 43201-2693

61. F. Bawel, c/o Phillips Engineering Company, 721 Pleasant Street, St. Joseph, MI 49085

62. E. W. Becker, Southern California Gas Company, P.O. Box 3249, Terminal Annex, Mail Location 731-D, Los Angeles, CA 90051

63. W. J. Biermann, 45 Foxcroft Drive, Fayetteville, NY 13066

64. U. Bonne, Honeywell Corporate Technology Center, 10701 Lyndale Avenue South, Boomington, MN 55420

65. B. G. Buchanan, Computer Science Department, University of Pittsburgh, 206 Mineral Industries Building, Pittsburgh, PA 15260

66. R. Cohen, Ray W. Herrick Laboratories, Purdue University, West Lafayette, IN 47907

67. D. D. Colosimo, Mechanical Technology, Inc., 968 Albany-Shaker Road, Latham, NY 12110

68. R. Crawford, Air Conditioning and Refrigeration Center, University of Illinois, 1200 W. Green Street, Urbana, IL 61801

69. J. Cuttica, Gas Research Institute, 8600 West Bryn Mawr Avenue, Chicago, IL 60631

70. K. Davidson, Gas Research Institute, 8600 West Bryn Mawr Avenue, Chicago, IL 60631

71. A. C. DeVuono, Battelle, Columbus Division, 505 King Avenue, Columbus, OH 43201-2693

72. D. A. Didion, National Institute of Standards & Technology, CBT, Gaithersburg, MD 20899

73. W. Dolan, Gas Research Institute, 8600 West Bryn Mawr Avenue, Chicago, IL 60631

74. D. C. Erickson, Energy Concepts Co., 627 Ridgely Ave., Annapolis, MD 21401

75. R. J. Fiskum, CE-422, 5H-048/FORS, U.S. Department of Energy, Washington, DC 20585

76. S. Freedman, Gas Research Institute, 8600 West Bryn Mawr Avenue, Chicago, IL 60631

77. C. French, Gas Research Institute, 8600 West Bryn Mawr Avenue, Chicago, IL 60631

78. T. Gilles, Lennox Industries Incorporated, P.O. Box 809000, Dallas, TX 75380-9000

79. J. C. Goldsmith, CE-332, 5H-041/FORS, U.S. Department of Energy, Washington, DC 20585

80. G. Grossman, Technion-Israel Institute of Technology, Faculty of Mechanical Engineering, Haifa 32000, Israel

81. M. E. Gunn, U.S. Department of Energy, CE-12/FORS, Washington, DC 20585

82. W. T. Hanna, Battelle Columbus Laboratories, 505 King Avenue, Columbus, OH 43201-2693

83. J. R. Harnish, Central Environmental Systems, York International Corporation, P.O. Box 1592-191B, York, PA 17405-1592

84. F. C. Hayes, The Trane Company, 3600 Pammell Creek Road, LaCrosse, WI 54601

85. K. E. Hickman, York International Corporation, P.O. Box 1592-191A, York, PA 17405-1592

86. A. Hirsch, Midwest Research Institute, 5109 Leesburg Pike, Suite 414, Falls Church, VA 22041

87. V. Jayaraman, Consolidated Natural Gas Service Co., CNG Towers, Pittsburgh, PA 15222-3199

88. P. Joyner, Electric Power Research Institute, P.O. Box 10412, Palo Alto, CA 94303

89. T. Kapus, Building Equipment Division, CE-422, 5H-048/FORS, U.S. Department of Energy, Washington, DC 20585

90. K. Kazmer, Gas Research Institute, 8600 West Bryn Mawr Avenue, Chicago, IL 60631

91. A. Lannus, Electric Power Research Institute, P.O. Box 10412, Palo Alto, CA 94303

92. R. A. Macriss, Phillips Engineering Company, 721 Pleasant Street, St. Joseph, MI 49085

93. J. Marsala, Gas Research Institute, 8600 West Bryn Mawr Avenue, Chicago, IL 60631

94. G. Melikian, United Technology Research Center, East Hartford, CT 06108

95. M. S. Menzer, American Gas Association, 1515 Wilson Boulevard, Arlington, VA 22209

96. J. P. Millhone, CE-13, 5E-080/FORS, U.S. Department of Energy, Washington, DC 20585

97. D. E. Morrison, 333 Oxford Road, East Lansing, MI 48823

98. R. Modahl, The Trane Company, 3600 Pammel Creek Road, LaCrosse, WI 54601-7599

99. K. P. Murphy, Allied-Signal, P.O. Box 1087 R, Morristown, NJ 07960

100. G. H. Myers, Gas Research Institute, 8600 West Bryn Mawr Avenue, Chicago, IL 60631

101. R. Nader, P.O. Box 19367, Washington, DC 20036

102. T. Occhionero, American Gas Cooling Center, 1515 Wilson Blvd., Arlington, VA 22209

103. D. Pellish, CE-332, 5H-041/FORS, U.S. Department of Energy, Washington, DC 20585

104. H. Perez-Blanco, 314 Mechanical Engineering Building, Pennsylvania State University, University Park, PA 16802

105. S. Petty, Columbia Gas System Service Corporation, 1600 Dublin Road, P.O. Box 2318, Columbus, OH 43215

106. B. A. Phillips, Phillips Engineering Company, 721 Pleasant Street, St. Joseph, MI 49085

107. B. Plzak, Refrigeration Systems Division, The Trane Company, 3600 Pammel Creek Road, LaCrosse, WI 54601-7599

108. R. Radermacher, University of Maryland, Mechanical Engineering Department, College Park, MD 20742

109. J. Rasson, Lawrence Berkeley Laboratory, 1 Cyclotron Road, Berkeley, CA 94720

110. E. A. Reid, Columbia Gas System Service Corporation, P.O. Box 2318, Columbus, OH 43215

111. R. C. Reimann, Carrier Corporation, 6304 Carrier Parkway, P.O. Box 4800, Syracuse, NY 13221

112. G. M. Reistad, Department of Mechanical Engineering, Oregon State University, Corvallis, OR 97331

113. H. H. Rhea, Lennox Industries, Inc., P.O. Box 877, Carrollton, TX 75006

114. U. Rockenfeller, Rocky Research, 674 Wells Road, Boulder City, NV 89005

115. J. D. Ryan, CE-422, 5H-048/FORS, U.S. Department of Energy, Washington, DC 20585

116. W. A. Ryan, Gas Research Institute, 8600 West Bryn Mawr Avenue, Chicago, IL 60631

117. P. Scheihing, CE-141, 5G-067/FORS, U.S. Department of Energy, Washington, DC 20585

118. S. V. Shelton, Thermax, Inc., 296 14th Street NW, Atlanta, GA 30318

119. H. O. Spauschus, Georgia Institute of Technology, Energy and Materials Sciences Laboratory, Atlanta, GA 30332

120. W. R. Staats, Gas Research Institute, 8600 West Bryn Mawr Avenue, Chicago, IL 60631

121. T. Statt, CE-422, 5H-048/FORS, U.S. Department of Energy, Washington, DC 20585

122. P. Swenson, Consolidated Natural Gas, CNG Tower, Pittsburgh, PA 15222-3199

123. D. Uselton, Lennox Industries, Inc., P.O. Box 877, Carrollton, TX 75011-0877

124. G. C. Vliet, Taylor Hall 116, The University of Texas, Austin, TX 78712

125. M. Wahlig, Lawrence Berkeley Laboratory, 1 Cyclotron Road, Berkeley, CA 94720

126. W. H. Wilkinson, Battelle Columbus Laboratories, 505 King Avenue, Columbus, OH 43201-2693

127. M. Williams, Department of Economics, Northern Illinois University, DeKalb, IL 60115

128. T. Zawacki, Phillips Engineering Company, 721 Pleasant Street, St. Joseph, MI 48095

129. Office of the Assistant Manager for Energy R&D, U.S. Department of Energy, Oak Ridge Operations, Oak Ridge, TN 37831

130-139. Office of Scientific and Technical Information, Department of Energy, P.O. Box 62, Oak Ridge, TN 37831